Polymer Chemistry

RSCPublishing

ARTICLE

Synthesis and Thermoresponsive Property of Four-Arm Star-Shaped Poly(*N*-isopropylacrylamide)s Bearing Covalent and Non-Covalent Cores

Cite this: DOI: 10.1039/x0xx00000x

Received 00th January 2015,
Accepted 00th January 2015,

DOI: 10.1039/x0xx00000x

www.rsc.org/

*Yougen Chen,[§] Nao Xiao,[†] Moe Fukuoka,[‡] Kohei Yoshida,[‡] Qian Duan,[¶] Toshifumi Satoh,[‡] Toyoji Kakuchi[§‡]**

The present study describes the precise synthesis and thermoresponsive properties of two types of four-arm star-shaped poly(*N*-isopropylacrylamide)s (PNIPAM), *i.e.*, the covalently linked one (**3**) and the non-covalently Ru(II)-chelated one (**5**). The atom transfer radical polymerization (ATRP) method was used to prepare the azido-terminated PNIPAM (**1**) arm using (2-azidoethyl)-2-chloropropionamide (AECP) as the initiator. **3** was subsequently prepared based on the click reaction of **1** with a multifunctional linker of tetra[(5-hexynyloyloxy)methyl]methane. For comparison, its linear counterpart **2** was also synthesized as a reference polymer by the same method using ethyl 5-hexynyloate. The four-arm star-shaped PNIPAM Ru complex **5**, on the other hand, was prepared by a click-to-chelate approach, which involves the click reaction of **1** with 2,6-diethynylpyridine to produce the macroligand of 2,6-bis(1-PNIPAM-1,2,3-triazol-4-yl)pyridine (**4**) and the chelating reaction of $RuCl_3$ with **4** to afford **5**. The thermoresponsive properties of the resulting polymers were investigated using a UV-vis spectrophotometer by measuring the optical transmittance of the polymer solution with varying solution temperature and the cloud point (T_c) at a 50% transmittance intensity in order to assess their thermoresponsive properties. The detailed thermoresponsive properties of these polymers, including the effects of the polymer terminal and core linkage and constituents of the four-arm star-shaped PNIPAMs on the T_c, were significantly described in the later part of this study.

Introduction

Thermoresponsive polymers, enabling the reversible thermo-induced phase transition and separation around a critical temperature denoted as the cloud point (T_c), have been attracting significant interest due to their wide and promising applications for different purposes, such as memory materials, sensing probes, and medicine vectors.[1-7] These applications are basically rooted in the sudden variation of the existing states of a thermoresponsive polymer in aqueous solution around either an upper critical solution temperature (UCST) or a lower critical solution temperature (LCST). Poly(*N*-isopropylacrylamide) (PNIPAM) was the first reported LCST-type thermoresponsive polymer and currently the most popular studied one in the field of "smart polymers" because its LCST is very close to body temperature, for which it has been expected to have applications in living bodies.[8] To date, many thermoresponsive polymers have been developed, including the UCST-types, such as poly(ethylene oxide), poly(vinyl methyl ether), alkyl-modified poly(vinyl alcohol), poly(2-hydroxyethyl methacrylate), polybetaines, poly(acrylic acid) and the like,[9] and the LCST-types, such as some of poly(*N*-alkyl (meth)acrylamide)s, poly(*N*-vinylalkylamide)s, poly(meth)acrylates, polyphosphoesters, poly(vinyl ether)s, polyethers, and poly(alkyloxide)s.[10]

For the LCST-type polymer, it homogeneously dissolves in solution at low temperature and exists in a hydrated random-coil form. When its solution is heated to a temperature around its T_c, its hydrated coils start to dehydrate along the polymer chain and form a dehydrated globule state (phase transition), immediately after which the dehydrated polymer globules tend to aggregate and precipitate (phase separation) due to the coil-to-globule transition.[11] In the last decade, many efforts have been devoted to clarifying the structure-thermoresponsivity and stimuli-thermoresponsivity relationships.[12-19] The structure variation can be the polymer composition, the terminal group, block sequence and the like, while the stimuli variation can point to the pH, ionic strength, etc. For instance, PNIPAM conventionally shows a T_c around 32 °C, while it has a tunable T_c from 34.8 °C to 44.6 °C by introducing various terminal groups, such as the hydrophobic moiety of a phenyl group and the hydrophilic moiety of an amino group.[15,16] As another example, the T_c of poly[oligo(ethylene glycol) methacrylate] could be readily tuned in the range of 9-90 °C by varying the length of

the oligo(ethylene glycol) (OEG) side chain and the comonomer composition of different types of OEG methacrylates.[11,20-22] Recently, the effect of the polymer architecture on the thermoresponsivity has also been an interesting research topic. For instance, Xu and Liu et al. reported that star and brush PNAPAM with compact arms exhibited a two-stage temperature-induced phase transition.[7] Whittaker et al. and Liu et al. independently reported the thermoresponsive properties of star-shaped PNIPAM while their results were very different from each other.[23,24] Therefore, a further investigation of the architectural effect still seems to be of great significance.

In this study, we designed two types of star-shaped PNIPAMs having different core compositions together with their linear PNIPAM precursors in order to systematically elucidate the effects of the terminal group, core linkage, and core composition on the thermoresponsive property. This study describes (1) the molecular design and synthesis of the two types of star-shaped PNIPAMs as well as their precursors by combining the use of the atom transfer radical polymerization (ATRP) method, click chemistry, and chelating chemistry, as shown in Scheme 1, (2) investigation of the effects of the terminal group and covalent and non-covalent core linkages on the thermoresponsive property, and (3) the effect of the core composition on the thermoresponsive property. The results of this study are expected to provide a more profound understanding of the thermoresponsive behavior of the star-shaped thermoresponsive polymers.

Experimental Section

Materials. *N*-Isopropylacrylamide (NIPAM) was provided by the Kohjin Co., Japan, and re-crystallized twice from hexane/toluene (10/3, v/v) prior to use. Tris[2-(dimethylamino)ethyl]amine (Me_6TREN) was supplied by the Mitsubishi Chemical Co., Japan, and distilled under reduced pressure from calcium hydride, then stored under argon. Copper(I) chloride (99.995%), pentaerythritol (> 99%), ruthenium(III) chloride ($RuCl_3$, 45-55% content), and ammonium hexafluorophosphate (> 95%) were purchased from the Aldrich Chemical Co., USA, and used without further purification. 4-Dimethylaminopyridine (DMAP, > 99%) was purchased from Wako Pure Chemical Industries, Ltd., Japan, and vacuum dried for one night prior to use. *N*,*N*,*N*′,*N*″,*N*″-Pentamethyldiethylenetriamine (PMDETA) was available from Tokyo Chemical Industry Co., Ltd., Japan, and used as received. Ethanol (> 99.5%) was purchased from the Japan Alcohol Corporation and distilled over CaH_2. Tetrahydrofuran (THF, > 99.5%; water content, < 0.001%) was purchased from Kanto Chemicals Co., Inc., and used as received. *N*-(2-Azidoethyl)-2-chloropropionamide (AECP), 5-hexynyloyl chloride, ethyl 5-hexynyloate and 2,6-diethynylpyridine were synthesized according to the literature.[14,25-27] All other chemicals were purchased from available suppliers and used without purification.

Measurements. The ^{1}H (400 MHz) and ^{13}C NMR (100 MHz) spectra were recorded by a JEOL JNM-A400II. Size exclusion chromatography (SEC) was performed at 40 °C using a Jasco high performance liquid chromatography (HPLC) system (PU-980 Intelligent HPLC pump, CO-965 Column oven, RI-930 Intelligent RI detector, and Shodex DEGAS KT-16) equipped with a Shodex Asahipak GF-310 HQ column (linear, 7.6 mm × 300 mm; pore size, 20 nm; bead size, 5 μm; exclusion limit, 4 × 10^7) in DMF containing lithium chloride (0.01 M) at the flow rate of 0.4 mL min^{-1}. The number-average molar mass ($M_{n,SEC}$) and dispersity (M_w/M_n) of the polymers were calculated on the basis of a polystyrene calibration.

Scheme 1. Synthetic routes of azido end-functionalized (**1**), linear (2), and four-arm star-shaped PINPAMs (**3**), together with 2,6-bis(1-PNIPAM-1,2,3-triazol-4-yl)pyridine (**4**) and four-arm star-shaped PNIPAM Ru(II) complex (**5**), based on ATRP method, click reaction, and chelating chemistry.

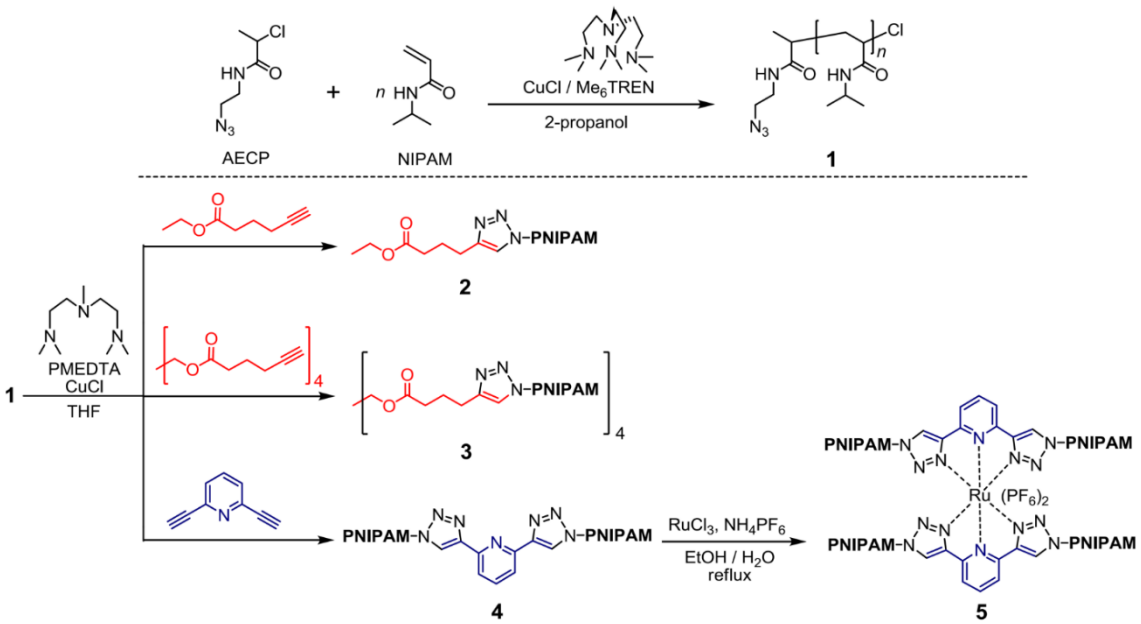

The preparative SEC was performed in THF (3.5 mL min^{-1}) at 23 °C using a JAI LC-9201 equipped with a JAI GEL-2H column (20 mm × 600 mm; exclusion limit, 5 × 10^3), a JAI GEL-3H column (20 mm × 600 mm; exclusion limit, 7 × 104) and a JAI RI-50s refractive index detector. The absolute molecular weight ($M_{w,SEC-MALS}$) was determined by size exclusion chromatography (SEC) in THF (1.0 mL min^{-1}) at 40 °C using an Agilent 1100 series instrument equipped with two Shodex KF-804L columns (linear, 8.0 mm × 300 mm; exclusion limit, 4 × 10^5; bead size, 7 μm), a DAWN 8 multi-angle laser light scattering (MALS) detector (Wyatt Technology, Santa Barbara, CA), a Viscostar viscosity detector (Wyatt Technology), and an Optilab rEX refractive index detector (Wyatt Technology). The IR spectra were recorded using a Perkin-Elmer Paragon 1000 FT-IR instrument. The cloud point measurements were performed on the ultraviolet-visible (UV-vis) spectra by passing a light source through a 10-mm path-length cell using a Jasco V-550 spectrophotometer equipped with an EYELA NCB-1200 temperature controller. The ultraviolet-visible (UV-vis) spectra of the polymer Ru(II) complexes were directly recorded by a Jasco V-550 spectrophotometer equipped with an EYELA NCB-1200 temperature controller at an aqueous solution concentration of 0.1 mg mL^{-1}.

Synthesis of tetra[(5-hexynyloyloxy)methyl]methane. To a mixture of pentaerythritol (220 mg, 1.62 mmol) and DMAP (0.786 g, 6.43 mmol) in dry dichloromethane (18 mL), 5-hexynyloyl chloride (1.00 g, 7.66 mmol) was slowly added at 0 °C under a nitrogen atmosphere and the mixture was stirred for 30 min at 0 °C. After the reaction mixture was stirred at room temperature for 4 days, the resulting salt was removed by filtration and the filtrate was washed with saturated *aq.* $NaHCO_3$, *aq.* NaCl, and distilled water. The organic layer was dried over anhydrous Na_2SO_4 and then evaporated to remove the solvent. The residue was purified by column chromatography (Silica gel, *n*-hexane/ethyl acetate = 3/1 (v/v), R_f = 0.26) to give the product as a light yellow viscous liquid. Yield, 410 mg (50%). ^{1}H NMR (400 MHz, DMSO-d_6, δ): 1.69 (8H, tt, J_1 = 7.3 Hz, J_2 = 14.5 Hz, -$CH_2CH_2CH_2$-), 2.19 (8H, dt, J_1 = 7.1 Hz, J_2 = 2.6 Hz, -CH_2C≡CH), 2.41 (8H, t, J = 7.5 Hz, -$CO_2CH_2CH_2$-), 2.80 (4H, t, J = 2.7 Hz, -CH_2C≡C*H*), 4.09 (8H, s, -CH_2O-). ^{13}C NMR (100 MHz, DMSO-d_6, δ): 17.01 (-*C*H_2C≡CH), 23.35 (-$CH_2CH_2CH_2$-), 32.32 (-CO*C*H_2-), 41.73 (*C*$(CH_2)_4$), 62.09 (-*C*H_2O-), 71.71 (-CH_2C≡*C*H), 83.53 (*C*≡CH), 171.94 (*C*=O) Anal. Calcd for $C_{29}H_{36}O_8$ (512.59): C, 67.95; H, 7.08. Found: C, 67.69; H, 7.21.

Synthesis of azido-terminated PNIPAM (1). A typical synthetic method is described as follows: to a stirrer-equipped three-neck flask, NIPAM (25.1 g, 221 mmol, 15 eq.) and CuCl (1.46 g, 14.7 mmol, 1.0 eq.) were dissolved in 2-propanol (40.0 mL). The mixture was degassed for 30 min by argon bubbling. To this mixture, a degassed stock solution of Me_6TREN in 2-propanol (8.43 mL, 1.74 mol L^{-1}, 14.7 mmol, 1.0 eq.) was added. Followed by a 10-min stirring, a degassed stock solution of AECP in 2-propanol (9.29 mL, 1.58 mol L^{-1}, 14.7 mmol, 1.0 eq.) was added to start the polymerization. The entire mixture was stirred for 4 h at room temperature and the polymerization was then quenched by bubbling air into the mixture. The mixture was passed through a short silica column using THF as the eluent to remove the copper catalyst. The polymer solution was concentrated, then reprecipitated into a large amount of *n*-hexane. The residue was filtered, and dried in vacuo for one night to give **1a** as a white soild. Yield, 16.5 g (66%). $M_{n,NMR}$ = 2,100 g mol^{-1}; $M_{n,SEC}$ = 3,000 g mol^{-1}, M_w/M_n(SEC) = 1.24; $M_{w,SEC-MALS}$ = 3,500 g mol^{-1}.

Synthesis of 4-[(3-ethyloxy)carbonyl]propyl-1*H*-1,2,3-triazolyl-terminated PNIPAM (2). Method A: in a 15-mL vial, ethyl 5-hexynyloate (63.8 mg, 0.455 mmol, 3.0 eq.), **1b** ($M_{n,NMR}$ = 3,300 g mol^{-1}, 500 mg, 0.152 mmol, 1.0 eq.), and CuCl (90 mg, 0.910 mmol, 6.0 eq.) were dissolved in THF (1.5 mL) and sealed using a rubber septum. After the entire mixture was bubbled with argon for 20 min, degassed PMDETA (158 mg, 0.910 mmol, 6.0 eq.) was injected into the vial. The click reaction was implemented for 40 h at room temperature and then quenched by bubbling air into the mixture. The mixture was passed through a short silica column using THF as the eluent to remove the copper catalyst. The polymer was purified by preparative SEC and lyophilized from the aqueous solution to give the linear PNIPAM of **2b** as a white solid. Yield, 225 mg (49%). $M_{n,NMR}$ = 3,760 g mol^{-1}; $M_{w,SEC-MALS}$ = 6,000 g mol^{-1}, M_w/M_n (MALS) = 1.13.

Synthesis of four-arm star-shaped PNIPAM (3). Method A was applied to **1b** ($M_{n,NMR}$ = 3,300 g mol^{-1}, 2.00 g, 0.928 mmol, 8.0 eq.), tetra[(5-hexynyloyloxy)methyl]methane (59.5 mg, 0.116 mmol, 1.0 eq.), CuCl (276 mg, 2.79 mmol, 24 eq.), PMDETA (964 mg, 5.57 mmol, 48 eq.), and THF (7.0 mL) for 24 h to give **3b** as a white solid. Yield, 65.0 mg (61%). $M_{n,NMR}$ = 14,700 g mol^{-1}; $M_{w,SEC-MALS}$ = 25,800 g mol^{-1}; M_w/M_n (MALS) = 1.17.

Synthesis of 2,6-bis(1-PNIPAM-1,2,3-triazol-4-yl)pyridine macroligand (4). Method A was applied to **1a** ($M_{n,NMR}$ = 2,100 g mol^{-1}, 800 mg, 0.381 mmol, 2.0 eq.), 2,6-diethynylpyridine (24.2 mg, 0.190 mmol, 1.0 eq.), CuCl (113 mg, 1.14 mmol, 6.0 eq.), PMDETA (395 mg, 2.28 mmol, 12 eq.), and THF (2.0 mL) for 72 h to give **4a** as a white solid. Yield, 600 mg (73%). $M_{n,NMR}$ = 4,900 g mol^{-1}; $M_{n,SEC}$ = 9,700 g mol^{-1}, M_w/M_n (SEC) = 1.10.

Synthesis of four-arm star-shaped PNIPAM Ru(II) complex (5). To a Schlenk flask containing ethanol/H_2O (7/1, v/v), $RuCl_3$ (10.8 mg, 52.0 μmol, 1.0 eq.) and **4a** ($M_{n,NMR}$ = 4,900 g mol^{-1}, 451 mg, 104 μmol, 2.0 eq.) were added under an nitrogen atmosphere. The mixture was refluxed for 18 h, then cooled to room temperature. NH_4PF_6 (170 mg, 1.04 mmol, 20 eq.) was added and the entire mixture was further stirred for another 10 min. The insoluble salt was removed by filtration. The product was purified by preparative SEC and lyophilized from an aqueous solution to give **5a** as a yellow

solid. Yield, 331 mg (70%). $M_{n,SEC}$ = 14,800 g mol^{-1}, M_w/M_n (SEC) = 1.11.

Cloud point (T_c) measurements. Typically, an aqueous solution of the polymer (2.0 g L^{-1}) was prepared, microwaved for 3 min, immersed into a 50 – 90 °C water-bath, and cooled in an ice bath for several min. The resulting clear solution was then filtered with a 0.45-μm PTFE membrane filter and transferred to a 10-mm length poly(methyl methacrylate) cell. The cell was kept under the initial determination temperature (**5**, 20 °C; other polymers, 30 °C) for 30 min. The transmittance of the aqueous solution at 500 nm was then recorded by a UV-vis spectrophotometer equipped with a temperature controller at the heating rate of 1.0 °C min^{-1}.

Results and discussion

Synthesis of four-arm star-shaped PNIPAM. In order to synthesize the star-shaped PNIPAM, the azido-terminated PNIPAM was initially prepared as the arm precursor for the subsequent click reactions. The atom transfer radical polymerization (ATRP) of NIPAM in 2-propanol at 20 °C was carried out for 3 – 6 h using *N*-(2-azidoethyl)-2-chloropropionamide (AECP) as the initiaor and CuCl/Me$_6$TREN as the catalyst system to prepare the azido-terminated PNIPAMs (**1a-1e**) under the conditions of [AECP]$_0$/[CuCl]$_0$/[Me$_6$TREN]$_0$ = 1/1/1 and NIPAM/2-propanol = 0.5 (w/w) unless instructed otherwise noted. The results are summarized in Table 1. The initial [NIPAM]$_0$/[AECP]$_0$ ratio was varied in the range of 15 – 275 in order to tune the molar mass of the PNIPAM arm. The polymerizations under such [NIPAM]$_0$/[AECP]$_0$ ratios afforded moderate to high monomer conversions of 69 – 97%, as estimated by the ^{1}H NMR measurements either in CDCl$_3$ or in D$_2$O. From the ^{1}H NMR measurements in D$_2$O, the molar masses ($M_{n,NMR}$s) of the resulting **1a-1e** were estimated to be in the range of 2,100 – 30,000 g mol^{-1}, each of which was slightly higher than its corresponding theoretical value calculated on the basis of the equation $M_{n,theo.}$ = (M.W. of NIPMA, 113.16) × Conv. × [NIPAM]$_0$/[AECP]$_0$ + (M.W. of AECP, 176.61), probably due to the cut-off of the low molar-mass polymers during the purification process by either reprecipitation or dialysis. On the other hand, those estimated by SEC measurements ($M_{n,SEC}$s) were in the range of 3,000 - 65,000 g mol^{-1} and obviously much higher than their related $M_{n,theo.}$s. This difference could be simply assigned to the mismatch between the synthesized **1** and the polystyrene standards. All the dispersities (M_w/M_ns) of **1a-1e** were reasonably situated in the range of 1.11 – 1.27 as the ATRP of NIPAM normally afforded. The structural information of **1** was verified by ^{1}H NMR and FT-IR measurements. For instance, the proton signals due to the -(C*H*$_2$)$_2$- at the initiation end of **1a** were clearly seen at 3.22 – 3.52 ppm together with those from the monomer units, as typically shown in Figure 1(a). From the FT-IR spectrum in Figure 2(a), the signals due to the stretching vibration of the azido group in **1a** apparently appeared at 2102 cm^{-1} together with those from the monomer units. For the other PNIPAM-N$_3$s, **1b-1e**, their chemical structures were also confirmed by the same method.

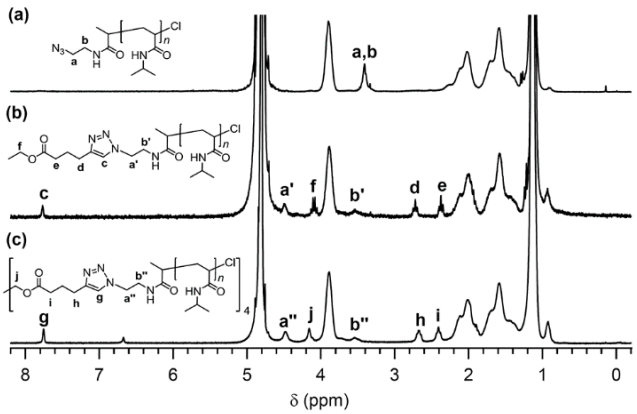

Figure 1. ^{1}H NMR spectra of (a) **1a**, (b) **2a**, and (c) **3a** in D$_2$O.

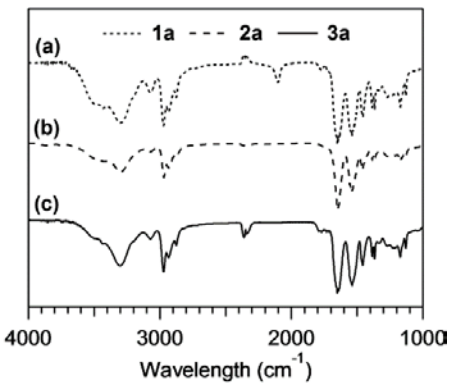

Figure 2. FT-IR spectra of (a) **1a**, (b) **2a**, and (c) **3a**.

The click reactions between **1a-1d** and tetra[(5-hexynyloyloxy)methyl]methane were implemented to prepare the covalently-bonded four-arm star-shaped PNIPAMs (**3a-3d**). For the

Table 1. Atom transfer radical polymerizations of NIPAM using AECP as an initiator in 2-propanol [a]

Polymer **1**	[NIPAM]$_0$ /[AECP]$_0$	Time (h)	Conv. (%) [c]	$M_{n,theo.}$ (g mol^{-1}) [d]	$M_{n,NMR}$ (g mol^{-1}) [e]	$M_{n,SEC}$ (g mol^{-1}) [f]	M_w/M_n [f]
1a	15	4	94 [e]	1,770	2,100	3,000	1.24
1b	25	4	97	2,900	3,300	5,300	1.18
1c	50	4	92	5,390	5,800	11,000	1.12
1d	100	3	69 [e]	8,000	11,000	20,000	1.11
1e [b]	275	5	79	24,800	30,000	65,000	1.27

[a] [AECP]/[CuCl]/[Me_6TREN] = 1/1/1; $[NIPAM]_0$/solvent = 0.5 (w/w); temp., 20 °C; 4 h. [b] $[NIPAM]_0$/solvent = 1 (w/w). [c] Determined by ^{1}H NMR in $CDCl_3$. [d] $M_{n,theo.}$ = 113.16 × Conv. × $[NIPAM]_0/[AECP]_0$ + 176.61. [e] Determined by ^{1}H NMR in D_2O. [f] Determined by SEC in DMF containing 0.01 mol·L^{-1} LiCl.

Table 2. Synthesis of linear (**2**) and four-arm star-shaped PNIPAM (**3**) by click chemistry using CuCl/PMEDTA in THF [a]

Azido end-functionalized PNIPAM (**1**)				Linear PNIPAM (**2**)				Four-arm star-shaped PNIPAM (**3**)			
	$M_{n,NMR}$ [a] (g mol^{-1})	$M_{w,SEC-MALS}$ [b] (g mol^{-1})	M_w/M_n [b]		$M_{n,NMR}$ [a] (g mol^{-1})	$M_{w,SEC-MALS}$ [b] (g mol^{-1})	M_w/M_n [b]		$M_{n,NMR}$ [a] (g mol^{-1})	$M_{w,SEC-MALS}$ [b] (g mol^{-1})	M_w/M_n [b]
1a	2,100	3,540	1.24	**2a**	2,560	3,580	1.26	**3a**	8,300	14,600	1.10
1b	3,300	5,560	1.13	**2b**	3,760	6,030	1.13	**3b**	14,700	25,800	1.17
1c	5,800	7,810	1.10	**2c**	6,120	8,120	1.05	**3c**	25,000	31,800	1.02
1d	11,000	21,400	1.06	**2d**	11,300	9,940	1.09	**3d**	46,700	80,700	1.14
1e	30,000	--	--	**2e**	31,900	34,900	1.06	--	--	--	--

[a] $[\mathbf{1}]_0$/[ethyl 5-hexynyloate]$_0$/$[CuCl]_0$/$[PMEDTA]_0$ = 1/3/6/6; $[\mathbf{1}]_0$/[tetra[(5-hexynyloyloxy)methyl]methane]$_0$/$[CuCl]_0$/$[PMEDTA]_0$ = 1/3/6/6; temp, r.t.. [b] Determined by ^{1}H NMR in D_2O. [c] Determined by SEC-MALLS in THF.

control experiments, the counterpart linear PNIPAMs (**2a-2e**) were also synthesized by the click reactions of **1a-1e** with ethyl 5-hexynyloate. To obtain the polymers as designed, a 2 × amount of **1** relative to that of the alkynyl group was used for preparing **3a-3d**, while a 3 × amount of ethyl 5-hexynyloate relative to that of **1** for **2**. After the click reactions, the unreactd **1** or ethyl 5-hexynyloate was removed by preparative SEC. The success of the click reaction for synthesizing **3** was verified by SEC measurements, as typically shown in Figure 3. The SEC trace of **3a** completely shifted to the high molar-mass region after the click reaction and no residual signal of **1a** was observed after purification by preparative SEC. Based on the molar-mass determintions either by ^{1}H NMR or by SEC-MALS (Table 2), the molar masses of **2a-2d**, as expected, were almost the same as their related precursors of **1a-1d** except for the absolute molar mass ($M_{w,SEC-MALS}$) of **2d** and those of **3a-3d** was exactly four times those of their corresponding **1a-1d**, though the $M_{w,SEC-MALS}$s for both **2** and **3** seemed to be overestimated. The click reactions were further verified by ^{1}H NMR and FT-IR measurements. In the ^{1}H NMR spectra of **2a** and **3a** (Figures 1(b) and 1(c)), the novel proton signals due to the cyclic triazole group were observed around 7.78 ppm along with those from the PNIPAM chains. Additionally, the signals at 3.30 – 3.52 ppm due to the methylene protons neighboring the azido group in **1a** fully shifted to 4.35 – 4.60 ppm after the click reaction. In the FT-IR spectra, the characteristic stretching signal of the azido group at 2102 cm^{-1} in **1a** completely disappeared after its click reaction with ethyl 5-hexynyloate or tetra[(5-hexynyloyloxy)methyl]methane, as shown in Figures 2(b) and 2(c). These investigations definitely suggested the successful preparation of **3a-3d** as well as their counterparts, **2a-2e**.

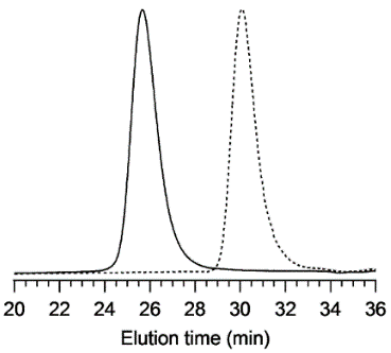

Figure 3. SEC traces of **1a** (dashed line) and **3a** (solid line).

Synthesis of four-arm star-shaped PNIPAM Ru(II) complex. Table 3 summarizes the synthetic results. **5** was prepared by the click-to-chelate approach according to our previous reports.[28,29] The macroligand of 2,6-bis(1-PNIPAM-1,2,3-triazol-4-yl)pyridine (**4**) was initially prepared by the click reaction of **1** with 2,6-diethynylpyridine at the initial feed ratio (molar ratio) of [2,6-diethynylpyridine]$_0$/$[\mathbf{1}]_0$ = 1/2. The detailed characteristics for **4** were followed by ^{1}H NMR, FT-IR, and SEC measurements like those for **2** and **3**, as depicted in Figures S1(b), S2(b), and S3(b). To obtain **5**, **4** was then chelated with $RuCl_3$ in EtOH/H_2O by refluxing the entire mixture at the $[\mathbf{4}]_0/[RuCl_3]_0$ = 2/1. Other impurities were removed by preparative SEC using THF as the eluent. After the chelating reaction, the four PNIPAM arms of **5** were non-covalently held together by the Ru(II)/2,6-bis(1,2,3-triazol-4-yl)pyridine (Ru(II)/*bitapy*) chelating core. The formation of **5** was confirmed by ^{1}H NMR and SEC measurements, *i.e.*, after the chelating reaction, the shift in the SEC trace to the high molar-mass region was clearly observed (Figure S3(c)) and the $M_{n,SEC}$ of **5** in Table 3 was almost twice that of its related macroligand **4**; in addition, in the ^{1}H NMR spectrum the shift and broadening phenomenon of the proton signals due to *bitapy* were seen (Figure S1(c)), which was due to the chelating interaction between Ru(II) and *bitapy*. We realized that the $M_{w,SEC-MALS}$ data of **5** should be more supportive for the formation of the star-shaped PNIPAM Ru complex. However, the exact $M_{w,SEC-MALS}$ data were not obtained because the SEC-MALS measurements in THF for such Ru(II) complexes made them aggregated and rendered significantly higher values perhaps due to their slight solubility after introducing the extremely polar Ru(II) cations. In addition to the ^{1}H NMR and SEC measurements, UV-Vis spectroscopy was also used to assess the optical properties of **5**, as shown in Figures 4. As a typical control spectrum, **4a** showed the maximum absorbance at 300 nm due to the electronic π-π^* transition of the *bitapy* moiety. After chelating, the above maximum absorbance obviously presented a blue shift to 286 nm and a new absorbance peak appeared around 390 nm due to

the metal-to-ligand charge transfer (MLCT) effect caused by the Ru(II)/*bitapy* complex core.[30] The MLCT effect, on the other hand, resulted in the slightly yellow color of the *aq*. **5a** solution. The molar absorptivity (ε_{MLCT} at MLCT absorbance) of **5a** in an *aq*. solution was in the range of 13,100 – 14,900, which was very consistent with the reported values of small Ru(II)/*bitapy* complexes.[31] The UV-Vis results once again supported the formation of the PNIPAM Ru(II) complex.

Table 3. Synthesis of 2,6-bis(1-PNIPAM-1,2,3-triazol-4-yl)pyridine (**4**) and four-arm star-shaped PNIPAM Ru(II) complex (**5**) [a]

Polymer **1**				Polymer **4**			Polymer **5**			
	$M_{n,NMR}$ [b] (g mol^{-1})	$M_{n,SEC}$ [c] (g mol^{-1})	M_w/M_n [c]		$M_{n,NMR}$ [b] (g mol^{-1})	M_w/M_n [c]		$M_{n,SEC}$ [c] (g mol^{-1})	M_w/M_n [c]	ε_{MLCT} (mol^{-1} cm^{-1})
1a	2,100	3,000	1.24	**4a**	4,830	1.22	**5a**	14,800	1.11	13,100
1b	3,300	5,300	1.18	**4b**	6,930	1.15	**5b**	24,700	1.10	13,800
1c	5,800	11,000	1.12	**4c**	9,820	1.09	**5c**	39,700	1.14	14,900

[a] [**1**]$_0$/[2,6-diethynylpyridine]$_0$/[CuCl]$_0$/[PMEDTA]$_0$ = 2/1/6/12; [**L**]$_0$/[$RuCl_3$]$_0$ = 2/1; Solvent, H_2O/ethanol; temp, reflux. [b] Determined by ^{1}H NMR in D_2O. [c] Determined by SEC in DMF containing 0.01 mol L^{-1} LiCl.

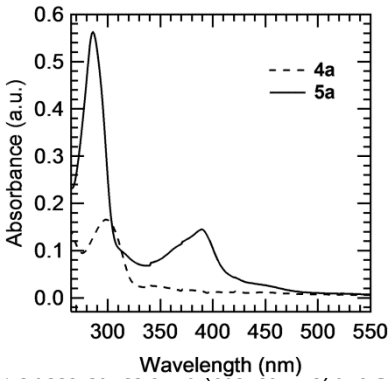

Figure 4. UV [illegible] (solid line).

Thermoresponsive property of four-arm star-shaped PNIPAM. The cloud point (T_c) in this study is defined as the temperature at which the optical transmittance of a polymer solution is located at a 50% intensity. The T_cs of all the polymer aqueous solutions were measured at a concentration of 2.0 g L^{-1} and a heating rate of 1.0 ^oC min^{-1}. All the T_cs of **1a-1e, 2a-2e**, and **3a-3d** are summarized in Table 4 and the dependence curves of their optical transmittance in an aqueous solution on temperature are shown in Figure 5(a). The transmittance of the polymer solutions exhibited a very abrupt decrease around the T_c for almost all of the polymers except for those of **1a**, **2a**, and **2b**. The sluggish decrease in transmittance of them could be simply due to their polydispersity effect, which is exacerbated in the low molar weight systems. This phenomenon had been frequently observed for thermoresponsive polymers with low molar masses in many other reports.[32,33] The T_cs of **1a**, **1b**, **1c**, **1d**, and **1e** were estimated to be 60.2, 51.1, 44.1, 41.0, and 35.8 ^oC, respectively; those of **2a**, **2b**, **2c**, **2d**, and **2e** were 55.6, 48.0, 43.2, 39.8, and 35.7 ^oC, respectively; and those of **3a**, **3b**, **3c**, and **3d** were 43.0, 39.0, 37.3, and 37.0 ^oC, respectively. No matter which type of polymer was considered, its T_c obviously decreased with the enhancement of molar mass. This molar-mass effect on its T_c has been very common and charateristic for the PNIPAM homopolymer.

In order to clarify the effect of the PNIPAM terminal group and covalent core linkage on the T_c, **2** is taken as the reference polymer for comparing the thermoresponsive properties of **1**, **2**, and **3**. When comparing the T_cs of **1** and **2**, the T_c of **1** was apparently higher than that of **2** under the premise they had the same molar mass. This difference could be rationally attributed to the well-known terminal effect of a linear PNIPAM *i.e.*, a hydrophilic terminal tends to enhance the T_c, while a hydrophobic one decreases the T_c.[14,15,18] The terminal effect is significantly observed especially when PNIPAM has a low molar mass. In our case, when **1** and **2** have the same molar mass, the only difference between them is that **1** possesses a hydrophilic azido moiety at the α-end, while **2** has a hydrophobic ester residue. Thus, the higher T_c of **1** versus **2** can be reasonably explained. On the other hand, the T_c difference became smaller with the increase in the molar mass and eventually negligible when the $M_{n,NMR}$ reached a value around 30,000 g mol^{-1}. This is because the terminal effect gets weaker with the increasing molar mass of a thermoresponsive polymer and can be eventually ignored when the molar mass is high enough, *e.g.*, 30,000 g mol^{-1} in this study. When comparing the T_cs of **3** and **2**, each of **3a-3d** had a lower T_c in contrast to its related linear counterpart **2** (equivalent to one PNIPAM arm of **3**), *i.e*, the T_cs of **3a**, **3b**, **3c**, and **3d** (43.0, 39.0, 37.3, and 37.0 ^oC, respectively) were markedly lower than those of their corresponding

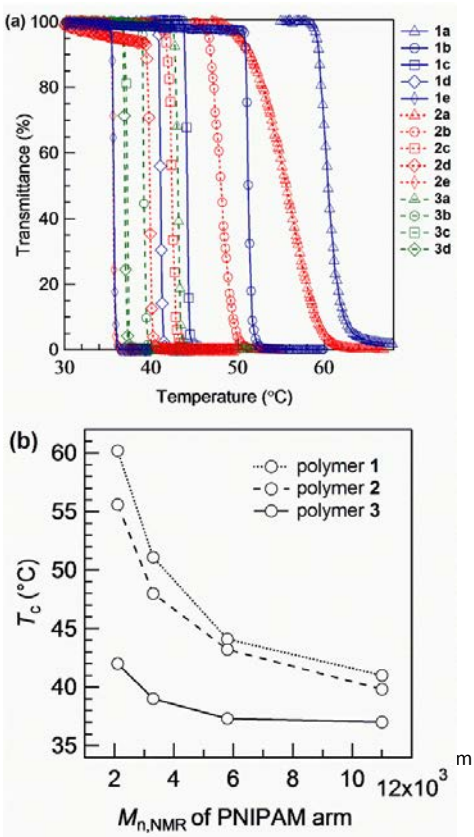

Table 4. A summarization of the cloud points (T_cs) of polymers **1**, **2**, **3**, **4**, and **5**

Polymer **1**			Polymer **2**			Polymer **3**			Polymer **4**			Polymer **5**		
	$M_{n,NMR}$ [a] (g mol^{-1})	T_c [b] (°C)		$M_{n,NMR}$ [a] (g mol^{-1})	T_c [b] (°C)		$M_{n,NMR}$ [a] (g mol^{-1})	T_c [b] (°C)		$M_{n,NMR}$ [a] (g mol^{-1})	T_c [b] (°C)		$M_{n,SEC}$ [c] (g mol^{-1})	T_c [b] (°C)
1a	2,100	60.2	**2a**	2,560	55.6	**3a**	8,300	43.0	**4a**	4,830	44.9	**5a**	14,800	43.0
1b	3,300	51.1	**2b**	3,760	48.0	**3b**	14,700	39.0	**4b**	6,930	41.1	**5b**	24,700	42.0
1c	5,800	44.1	**2c**	6,120	43.2	**3c**	25,000	37.3	**4c**	9,820	38.6	**5c**	39,700	38.1
1d	11,000	41.0	**2d**	11,300	39.8	**3d**	46,700	37.0	--	--	--	--	--	--
1e	30,000	35.8	**2e**	31,900	35.7	--	--	--	--	--	--	--	--	--

[a] Determined by ^{1}H NMR in D_2O. [b] Determined by UV-vis spectrophotometer equipped with a temperature controller at the heating rate of 1.0 °C min^{-1}. [c] Determined by SEC in DMF containing 0.01 mol L^{-1} LiCl.

Figure 5. (a) The transmittance dependence on temperature and (b) the T_c dependence on $M_{n,NMR}$ of the PNIPAM arm for polymers **1**, **2**, and **3** in aqueous solutions.

2a, **2b**, **2c**, and **2d** (55.6, 48.0, 43.2, and 39.8 °C, respectively). Given that the mass concentrations for the T_c determination are the same and the only structural difference between **2** and **3** is that the four PNIPAM arms of **3** are covalently linked, it is quite clear that the covalent linkage has a crucial effect on the thermoresponsive property. This effect is particularly significant when the molar mass of **3** is low. The covalent linkage at the core makes the T_c decrease because it helps to enhance the chain entanglement among the PNIPAM arms and results in the dehydration of the PNIPMA chains at a lower temperature, namely a lower T_c. The dependence of T_c on the $M_{n,NMR}$ of the PNIPAM arm is summarized in Figure 5(b). When **1**, **2**, and **3** had the same PNIPAM arm, **1** possessing the azido terminal showed the highest T_c and the covalently linked **3** showed the lowest value. There is no doubt that both the terminal group and core linkage affect the thermoresponsive property of PNIPAM.

Thermoresponsive property of four-arm star-shaped PNIPAM Ru(II) complex. In addition to the covalently bonded **3**, the thermoresponsive property of the non-covalently linked **5** was also investigated. The thermoresponsive behaviors of **5** and its precursor macroligand **4** were first compared to investigate the effect of the chelated Ru(II) cation on the T_c. As shown in Figure 6(a), the transmittance of the **5** solution displayed a clearly slower decreasing trend in comparison to its related precursor macroligand, especially when **5** had a low molar mass. This should be assigned to the introduction of the positively charged Ru(II), which leads to a more difficult aggregation of the positively charged PNIPAM globules obtained after the phase transition, due to the mutual exclusion interaction and stabilization and solvation effects of the Ru(II) cations. The T_cs for **5a**, **5b**, and **5c** were 43.0, 42.0, and 38.1 °C, respectively, and those of **4a**, **4b**, and **4c** were 44.9, 41.1, 38.6 °C, respectively, as shown in Figure 6(b). It seems difficult to find a common regularity in the T_c change between **5** and its corresponding **4**. Taking **4** as the reference, two factors can be considered to affect the thermoresponsive property of **5**. One is the cationically charged hydrophilic Ru(II)/*bitapy* core, which enhances the solvation of **5** and helps to increase the T_c. The other is the effect of the core linkage, which prefers to decrease the T_c, as observed for **3**. Therefore, they should be comprehensively brought into consideration and the balance of these two factors should be the key to explain the T_c difference between **5** and its related macroligand **4**. For instance, the T_c of **5** performs to be higher than that of **4** when the first factor plays the dominating role, otherwise, the T_c of **5** tends to be lower when the second factor dominates the entire thermoresponsivity.

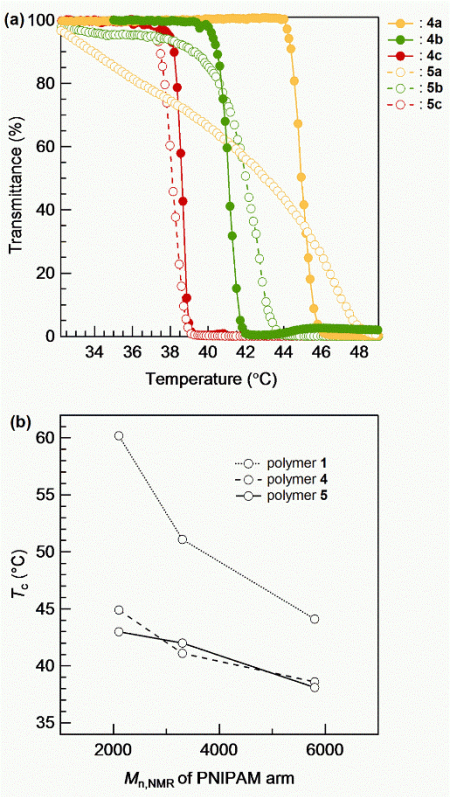

Figure 6. (a) The transmittance dependence on temperature for polymer **5** and its macroligand **4** in aqueous solutions and (b) (b) the T_c dependence on $M_{n,NMR}$ of the PNIPAM arm for polymers **1**, **4**, and **5** in aqueous solutions.

The thermoresponsive properties of **3** and **5** with the same molar mass were eventually compared in order to investigate how the core constitution affects the T_c, as shown in Figure 7. As observed, **5** generally exhibited a slightly higher T_c than those of **3** when they have the same PNIPAM arms. For instance, the T_cs of **5a**, **5b**, and **5c** were 43.0, 42.0, and 38.1 °C, while those of **3a**, **3b**, and **3c** were 43.0, 39.0, and 37.3 °C, respectively. This should be due to the difference in the hydrophilicity between the two cores, *i.e.*, the hydrophilic Ru(II)/*bitapy* core is prone to increase the T_c and the hydrophobic covalent core in **3** tends to decrease the T_c. Miyashita et al. previously investigated the thermoresponsive behavior of the PNIPAM that was randomly incorporated with a small amount of either hydrophobic pyrene moieties or hydrophilic Ru(II)/bipyridine complexes in the side chains. They found that during the coil-to-globule transition of the PNIPAM chains, the hydrophobic pyrenes were rigidly embedded into the hydrophobic polymer matrix in the globular state, while the hydrophilic Ru(II)/bipyridine complexes were located at the interface of the polymer globules to stabilize these hydrophobic globules by electron transfer quenching experiments.[34] Considering that their system is rather similar to ours, this explanation should be more or less suitable for our case, *i.e.*, the hydrophilic Ru(II)/*bitapy* were located at the interface of **5** after the phase transition and played the role of a stabilizer, which resulted in the slightly higher T_c than **3** even when they have the same PNIPAM arms.

Given that the addition of a salt to the PNIPAM solution could affect the T_c,[2] we also carried out the T_c measurements of the **3** aqueous solution in which an equimolar Ru(III)Cl_3 relative to Ru(II)$(PF6)_2$ was added, as shown in Figure S3. The reason why Ru(III)Cl_3, rather than Ru(II)$(PF6)_2$, was used is that Ru(II)$(PF6)_2$ was commercially unavailable. Obviously, there was no distinct T_c difference (0.2 °C) between the samples with and without adding Ru(III)Cl_3. This result indicates that the T_c difference was actually caused by the core composition, rather than the addition of the Ru(II) or Ru(III) salt.

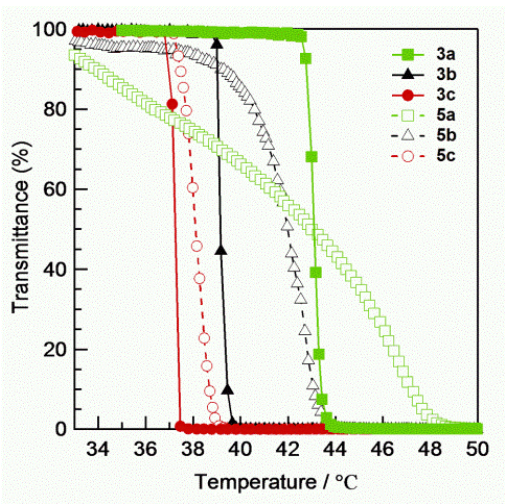

Figure 7. The transmittance dependence on temperature for polymers **3** and **5** in aqueous solutions.

Conclusion

We succeeded in preparing two types of four-arm star-shaped PNIPAMs, in which one was covalently bonded and the other was non-covalently linked through the chelating interaction of Ru(II)/*bitapy*, together with their linear precursors based on the ATRP method, click reaction, and chelating chemistry. Their thermoresponsive properties were then investigated and clarified. The effect of the terminal group on the T_c turned out to be very similar as previously reported by comparing the thermoresponsive behaviors of the azido end-functionalized (**1**) and linear PNIPAMs (**2**), *i.e.*, under the premise of the same molar mass, a hydrophilic terminal tends to enhance the T_c, while a hydrophobic one tends to decrease T_c. The effect of the core linkage on the T_c was studied by comparing the thermoresponsive behaviors of **2** and the four-arm star-shaped PNIPAM (**3**) and those of 2,6-bis(1-PNIPAM-1,2,3-triazol-4-yl)pyridine (**4**) and the four-arm star-shaped PNIPAM Ru(II) complex (**5**), from which the hydrophobic covalent linkage certainly decreased the T_c, while the hydrophilic Ru(II)/*bitapy* had no explicit influence on the T_c since two adversely influential factors including the linkage effect and charge effect need to be considered in this situation. Finally, the effect of the core composition on the T_c was investigated by comparing the thermoresponsive behaviors of **3** and **5**. The four-arm star-shaped PNIPAM with a hydrophilic core obviously showed a higher T_c mainly because the Ru(II)/*bitapy* complexes were located at the interface of the PNIPAM globules formed after the phase transition and thus stabilize the PNIPAM globules. As a result of this study, the authors expect the results in this study can provide useful information in designing thermoresponsive polymers.

Acknowledgment.

This work was financially supported by the MEXT (Japan) program "Strategic Molecular and Materials Chemistry through Innovative Coupling Reactions" of Hokkaido University and the MEXT Grant-in-Aid for Scientific Research on Innovative Areas "Advanced Molecular Transformation by Organocatalysts".

Notes and references

§ *Frontier Chemistry Center, Faculty of Engineering, Hokkaido University, Sapporo, 060-8628, Japan.*

† *School of Chemical Biology and Pharmaceutical Sciences, Capital Medical University, No. 10, You'an Men, Waixi Toutiao, Beijing, 100069, China.*

‡ *Division of Biotechnology and Macromolecular Chemistry, Faculty of Engineering, Hokkaido University, Sapporo, 060-8628, Japan.*

¶ *School of Materials Science and Engineering, Changchun University of Science and Technology, Changchun 130022, China*

Corresponding author: kakuchi@poly-bm.eng.hokudai.ac.jp

† Electronic Supplementary Information (ESI) available: The data for ^{1}H NMR and FT-IR spectra of **4a** and **5a** and the

transmittance curves of **3b** before and after adding $RuCl_3$ are available. See DOI: 10.1039/b000000x/

1 M. A. Ward and T. K. Georgiou, *Polymers* 2011, **3**, 1215-1242.
2 H. G. Schild, *Prog. Polym. Sci.*, 1992, **17**, 163-249.
3 S. Ohya and T. Matsuda, *J. Biomater. Sci. Polymer Edn.*, 2005, **16**, 809-827.
4 T. Mori, D. Umeno and M. Maeda, *Biotech. Bioengi.*, 2001, **72**, 261-268.
5 S. Mias, J. Sudor and H. Camon, *Microsyst. Technol.*, 2008, **14**, 691-695.
6 D. Schmaljohann, *Adv. Drug Deliv. Rev.*, 2006, **58**, 1655-1670.
7 R. Liu, M. Fraylich and B. R. Saunders, *Colloid Polym. Sci.*, 2009, **287**, 627-643.
8 J. S. Scarpa, D. D. Muller and I. M. Klotz, *J. Am. Chem. Soc.*, **1967**, *89*, 6024-6030.
9 J. Seuring and S. Agarwal, *Macromol. Rapid Commun.*, 2012, **33**, 1898-1920.
10 D. Roy, W. L. A. Brooks and B. S. Sumerlin, *chem. Soc. Rev.*, **2013**, *42*, 7214-7243.
11 V. Aseyev, H. Tenhu and F. M. Winnik, *Adv. Polym. Sci.*, 2010, **242**, 29-89.
12 H. Y. Liu and X. X. Zhu, *Polymer* 1999, **40**, 6985-6990.
13 X. P. Qiu, T. Koga, F. Tanaka and F. M. Winnik, *Sci. China Chem.*, 2013, **56**, 56-64.
14 A. Narumi, K. Fuchise, R. Kakuchi, A. Toda, T. Satoh, S. Kawaguchi, K. Sugiyama, A. Hirao and T. Kakuchi, *Macromol. Rapid Commun.*, 2008, **29**, 1126-1133.
15 Y. Xia, A. D. Burke and H. D. H. Stöver, *Macromolecules* 2006, **39**, 2275-2283.
16 R. K. Iha, K. L. Wooley, A. M. Nyström, D. J. Burke, M. J. Kade and C. J. Hawker, *Chem. Rev.*, 2009, **109**, 5620-5686.
17 Y. Xia, X. Yin, A. D. Burke and H. D. H. Stöver, *Macromolecules* 2005, **38**, 5937-5943.
18 J. E. Chung, M. Yokoyama, T. Aoyagi, Y. Sakurai and T. Okano, *J. Control. Release* 1998, **53**, 119-130
19 D. G. Lessard, M. Ousalem and X. X. Zhu, *Can. J. Chem. Soc.*, 2001, **79**, 1870-1874.
20 J.-F. Lutz and A. Hoth, *Macromolecules* 2006, **39**, 893-896.
21 S. Han, M. Hagiwara and T. Ishizone, *Macromolecules* 2003, **26**, 8312-8319.
22 J.-F. Lutz, Ö. Akdemir and A. Hoth, *J. Am. Chem. Soc.*, 2006, **128**, 13046-13047.
23 R. Plummer, D. J. T. Hill and A. W. Whittaker, *Macromolecules* 2006, **39**, 8379-8388.
24 J. Xu, and S. Liu, *J. Polym. Sci., Part A: Polym. Chem.*, 2009, **47**, 404-419.
25 R. Luxenhofer and R. Jordan, *Macromolecules* 2006, **39**, 3509-3516.
26 M. Nakatani, Y. Fukunaga, H. Haraguchi, M. Taniguchi and T. Hase, *Bull. Chem. Soc. Jpn.*, 1986, **59**, 3535-3539.
27 T. Kawano, T. Kato, C. X. Du and I. Ueda, *Tetrahedron Lett.* 2002, **43**, 6697-6700.
28 N. Xiao, Y.-G. Chen, X.-D. Shen, C.-H. Zhang, S. Yano, M. Gottschaldt, U. S. Schubert, T. Kakuchi and Satoh, T. *Polym. J.* 2012, **45**, 216-225.
29 Y.-G. Chen, N. Xiao, T. Satoh and T. Kakuchi, *Polym. Chem.* 2014, **5**, 4993-5001.
30 J. T. Fletcher, B. J. Bumgarner, N. D. Engles and D. A. Skoglund, *Organometallics* 2008, **27**, 5430-5433.
31 B. Schulze, C. Friebe, M. D. Hager, A. Winter, R. Hoogenboon, H. Gorls and Schubert, U. S. *Dalton Trans.*, 2009, **38**, 787-794.
32 Y. Tsuboi, T. Tada, T. Shoji and N. Kitamura, *Macromol. Chem. Phys.*, 2012, **213**, 1879-1884.
33 Y. Tsuboi, K. Kikuchi, N. Kitamura, H. Shimomoto, S. Kanaoka and S. Aoshima, *Macromol. Chem. Phys.*, 2012, **213**, 374-381.
34 T. Taniguchi, M. Kuroki and T. Miyashita, *Colloid. Polym. Sci.*, 1996, **274**, 717-722.

For Table of Contents Graphical Abstract Use Only

Synthesis and Thermoresponsive Property of Four-Arm Star-Shaped Poly(*N*-isopropylacrylamide)s Bearing Covalent and Non-Covalent Cores

*Yougen Chen,[§] Nao Xiao,[†] Moe Fukuoka,[‡] Kohei Yoshida,[‡] Qian Duan,[¶] Toshifumi Satoh,[‡] Toyoji Kakuchi[§‡]**

We succeeded in synthesizing a series of poly(*N*-isopropylacrylamide)s with linear and four-arm star-shaped structures and clarified their thermoresponsive properties.